

Low Emittance Transport Studies for the Alignment of the International Linear Collider

Theodor D. Braşoveanu

*Department of Physics and Astronomy,
Vanderbilt University, Nashville, TN 37235*

(Dated: August 12, 2005)

The International Linear Collider (ILC) will be a new 33 km long 500 GeV center of mass linear accelerator that will collide electron and positron bunches together at unprecedented luminosity. Critical to preserving the very high luminosity is a very small transverse beam size (or emittance). This requires an alignment precision within microns of the accelerator components along the entire length of the linac. Since site survey can only align components to hundreds of microns at the most, more sophisticated alignment methods are required that rely on the accelerated beam as the diagnostic tool. Essential to these *Beam-Based Alignment* techniques is precise measurement of the beam position along the length of the linac using Beam Position Monitors (BPMs). The main purpose of our studies has been to determine the BPM resolution required to adequately maintain the beam emittance. To reach this objective, we performed computer simulations of the acceleration of an electron bunch through the linac, which enabled us to test, compare and improve the effectiveness of three alignment algorithms.

I. INTRODUCTION

In view of the exotic physics phenomena that the ILC is hoped to investigate, such as the Higgs bosons and, possibly, supersymmetry, a very high luminosity ($10^{34} \text{ cm}^{-2} \text{ s}^{-1}$) has to be maintained at the interaction point. A high luminosity maximizes the rate of head-on collisions necessary for particle interactions, so the luminosity factor is a measure of the interaction probability in the colliding beams and is directly related to the transverse beam dimensions or the transversal cross-section, as given by [1]:

$$L = \frac{1}{4\pi} \frac{fN_1N_2}{\sigma_x\sigma_y} \quad (1)$$

where L is the luminosity, f is the bunch crossing rate, N_1 and N_2 are the number of particles in each of the colliding beams, whereas σ_x and σ_y are the horizontal and vertical rms beam sizes.

Another quantity, called emittance, is a good measure of the beam size. Defined as the square of the constant amplitude factor in the position-dependent transverse oscillations (known as betatron oscillations) about the orbit described by the trajectory of a beam particle, the emittance is an invariant of the particle motion, equal within a factor of π to the area A of the phase space ellipse described by the particle in the x - x' or y - y' plane: $\epsilon = A/\pi$ [1]. This is a consequence of Liouville's Theorem, which predicts that the shape and position of the ellipse might change as the particle moves along the orbit but the area, and therefore the emittance, will nevertheless remain constant. For an assembly of many particles, the average projected emittance of the beam is a more appropriate quantity, since it assumes the statistical distribution of all the particles tracked in a bunch [2]:

$$\epsilon_{RMS} = (\langle x^2 \rangle \langle x'^2 \rangle - \langle xx' \rangle^2)^{1/2} \quad (2)$$

This corresponds to the average projected horizontal emittance, while a similar version for the average projected vertical emittance (in y, y' form) is available as well. With no misalignments in either the beam or the linac lattice, the standard normalized vertical emittance in the linac is about 20 nm. The (relativistic) normalization factor is $\beta\gamma$ and has been applied to compensate for the energy dependence of ϵ_{RMS} . The 20 nm value is the design emittance provided by the bunch compressor at the point where the beam is injected into the linac.

Misalignment of either the beam or the lattice elements (quadrupoles, RF cavities) can cause undesired phenomena such as wakefields, filamentation and dispersive kicks [2], which can all lead to beam instabilities and emittance dilution. Therefore, various beam-based alignment algorithms, including Ballistic Alignment, Kubo Method and Dispersion Free Steering, have been proposed to reduce the sources of emittance dilution, realign the beam and preserve the vertical emittance within a 100% budget [3].

All the simulations have been carried out with TAO (Tools for Accelerated Optics), a software developed at Cornell University based on the Bmad relativistic charged-particle dynamics library [4]. It allows one to design lattices subject to constraints, perform lattice corrections or simulate errors and changes in machine parameters. A beam of 250 particles in a gaussian distribution is used in the tracking simulations and the initial normalized vertical emittance is set to 20 nm. The emittance along the orbit is then calculated from distributions that match the design values for both the horizontal and vertical emittance, upon rescaling the bunch parameters. Our goal has been to find the necessary alignment precision, such that a small emittance is maintained throughout the linac, from the extraction of the damping rings to the interaction point.

II. TESTING THE BEAM-BASED ALIGNMENT ALGORITHMS

A more in-depth description of the BBA methods used can be found in [3].

Ballistic Alignment (BA) follows closely the implementation given in [5]. The lattice is divided into bins of interconnected FODO cells, with each cell containing 2 quadrupoles and 2 corresponding BPMs, and the beam is allowed to take a ballistic path, under the influence of gravity only. The reference line for the path is established by switching off all quadrupoles of a bin, while the beam is centered in the last BPM of the bin. The ultra-relativistic velocities of the particles would turn this path into an almost straight line, as recorded by the BPMs. After the quadrupoles have been switched back on, the beam is re-steered to the other BPMs such that their centers fall onto the measured ballistic orbit.

Dispersion Free Steering (DFS) follows the version developed by [6]. The trajectory is measured and adjusted to minimize dispersion. Prior to performing the alignment, the beam is steered to zero the BPMs. The linac is then divided into regions of 20 FODO cells, with each region overlapping its neighbor by 10 cells. Two orbits of different energies are considered for each region and a Levenberg-Marquardt optimizer is used to find the correction parameters needed to minimize the orbit difference between the on- and off-state. Upon improvements performed on DFS, caution in perfectly aligning the first quadrupoles and corresponding BPMs, as well as further re-steering the incoming orbit, is no more an issue of concern. Instead, Ballistic Alignment is performed on the first 3 quadrupoles

(compare with [3]).

The *Kubo Method* allows removing the dispersion from misaligned quadrupoles by adjusting each steering magnet to exactly cancel the quadrupole kick. Prerequisite for applying the correction is knowledge of the BPM to quadrupole offset, so the algorithm assumes that quadrupole shunting (measuring the beam kick vs. quad strength to determine the offset) has been performed and gives an estimate of 30 microns for the rms BPM to quad offset. The difference to the original version [7,8] lies in applying the correction linearly from the beginning to the end of the lattice. The kick on a steering magnet is given by:

$$\theta = w\theta_{bpm} + k_1 L_{quad} Y_{bpm} \quad (3)$$

where w is the weighting factor, θ_{bpm} is the kick that would be placed on the magnet to zero the orbit at the next BPM, k_1 and L_{quad} are the quadrupole strength and length and Y_{bpm} is the BPM reading.

To test the three above-mentioned alignment algorithms, we first applied the full set of design misalignments featured in [6,9] and in Table I. These are the ab initio/nominal installation conditions and are a good measure for the design tolerances. Studies on the dependence of the vertical emittance on individual misalignment sources have been made [10], in order to estimate the emittance growth due to misalignment of particular components of the lattice. The following table features different types of misalignments and the relevant tolerance levels set partly by the TESLA design, together with values for the normalized vertical emittance corresponding to large misalignments, at twice the tolerance level (given in the rightmost column of Table I). The reader should refer for comparison to the similar study outlined in [2].

TABLE I: The ILC Design Misalignments.

Misalignment	Relative to	Tolerance level	Emittance value (2x tolerance)
quad offset	cryostat	300 μm	3 mm
quad tilt	cryostat	300 μrad	30 nm
RF cavity offset	cryostat	300 μm	35 nm
RF cavity pitch	cryostat	200 μrad	11 μm
cryostat offset	survey line	200 μm	1.3 mm
cryostat pitch	survey line	20 μrad	1.6 μm
BPM offset	cryostat	300 μm	20 nm (no change)
BPM resolution	true orbit	10 μm	given in Section III

With the complete set of misalignments applied for single bunch tracking, assuming no incoming jitter, no stray fields (either external or residual from the magnets) and no ground motion, we found the following values for the final vertical emittance, averaged over 100 seeds: 24.3 ± 0.22 nm in case of Ballistic Alignment using a standard of 7 cells/bin, which closely matches the similar study reported in [3]; 31.2 ± 0.61 nm for Dispersion Free Steering using a standard of 20 cells/region with 10 cell overlap, which is considerably less than the value cited in [3], due to recent improvements in the algorithm; 35.7 ± 1.24 nm in case of Kubo using the 30 μm suggested BPM to quad offset, which is again an improvement compared to [3]. However, it should be noted that the issue of wakefields, which are produced by image currents in the cavities, has not been fully handled by TAO,

until recently. Therefore, future simulations are expected to result in slightly higher values for the emittance in all three cases.

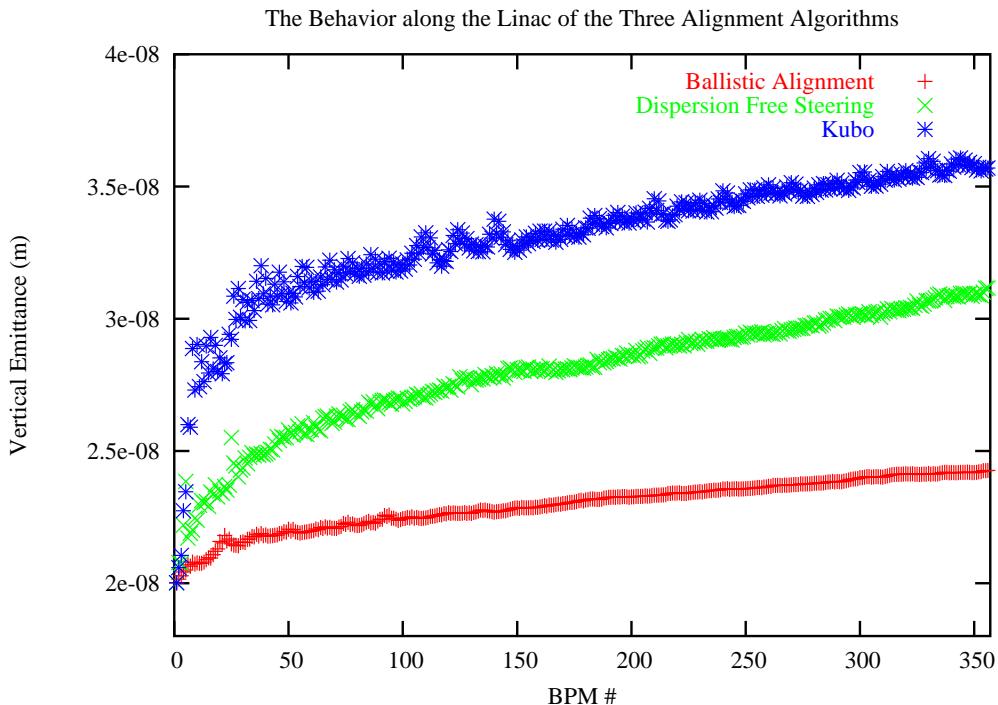


FIG. 1: This tracks the emittance throughout the linac lattice while running the alignment routine for 100 seeds within the design misalignments.

Figure 1 gives an insight into how the normalized vertical emittance changes throughout the linac after the misalignments have been applied and the alignment algorithms have been run to realign the beam. As it turns out, most of the increase in emittance occurs in the first part of the linac (first 50 BPMs). This is also the region where most fluctuations can be detected. For this reason, further sensitivity studies such as the effect of BPM resolution should pay particular attention to this first part of the linac. For the final emittance, the reader should refer for comparison to previous analyses [5, 6, 7, 8, 11].

III. STUDIES OF BPM NOISE RESOLUTION AND TILT

The role of the Beam Position Monitors is to read the particle position, by determining the displacement of the particle from the central axis, which is inferred from the charge induced by the particle on four electrode plates. By default in TAO all 355 BPMs (+ 1 virtual BPM placed at the end of the linac) have a $10 \mu\text{m}$ rms resolution, which is exactly the tolerance given in [5]. Since improvements in the technology used might reduce this number to a couple of μm , we chose to investigate how our three Beam-Based Alignment algorithms are affected by changes in the monitors' resolution, in an effort to complete the analysis started in [3, 11].

As shown in Figure 2, both BA and DFS feature a 20 to 30 % increase in the final normalized vertical emittance in the range of 0 to $20 \mu\text{m}$ BPM resolution, whereas Kubo doesn't seem to be affected at all in this range. An important conclusion is that the emittance

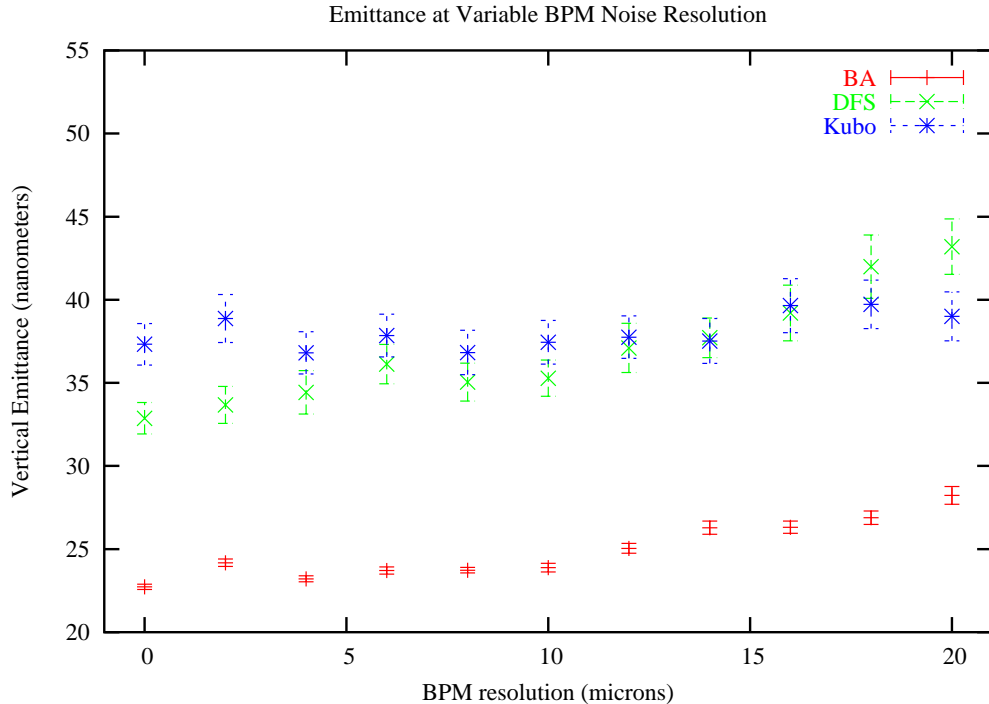


FIG. 2: The effect of variable BPM resolution on the emittance is given, including the mean and mean error for 100 seeds.

stays in most cases within the proposed budget (up to 40 nm), with the exception of DFS at above $18\mu\text{m}$ resolution. For a particularly bad resolution of $100\mu\text{m}$, we measured an emittance in the range of hundreds of nm for all 3 algorithms, which suggests that the increase is roughly linear, though significantly slower for Kubo.

The explanation for the different sensitivities of the three BBA algorithms used lies in the different treatments of the orbit. From the fact that DFS measures the difference in orbit between a high and a low energy orbit and does not take into account the absolute orbit of the particle, a BPM resolution in the range of tens of microns is closer in magnitude to this difference and causes greater disturbances in the alignment. The higher percent increase in the vertical emittance for DFS confirms this argument. In a similar but not identical fashion, BA, the next sensitive algorithm, uses a difference orbit as opposed to the absolute orbit, since it continuously adjusts the quadrupoles in the lattice to match the ballistic orbit, bin by bin. Thus, the offset in position will again be reduced and consequently brought closer to the BPM noise resolution range. The Kubo method, however, does not measure differences between orbits; it uses only one orbit measurement and the kicks on the magnets will not constrain this orbit, making it less sensitive to the noise in the BPMs.

An important question is whether all BPMs need to have the same noise resolution, or conversely, certain particularities are allowed for the beginning/end of the linac. To deal with this problem, we chose to adjust the BPM noise at the start of the linac to a very good resolution ($1\mu\text{m}$), with the rest of the BPMs set at $20\mu\text{m}$ resolution. The plot in Figure 3 shows that only having the first 50 BPMs providing high-precision readings is enough to keep the vertical emittance to values close to the ones obtained when the whole linac is set at $10\mu\text{m}$ resolution. Note that, in case of BA and DFS, the emittance steadily decreases as the region of $1\mu\text{m}$ resolution BPMs is extended, while Kubo shows again little or no

response to changes in resolution. Therefore, one has to worry less about having an entire linac built with high-precision BPMs and focus more on the first part of the linac, since this is the region where misalignments can have the most dramatic effects on the particles' position.

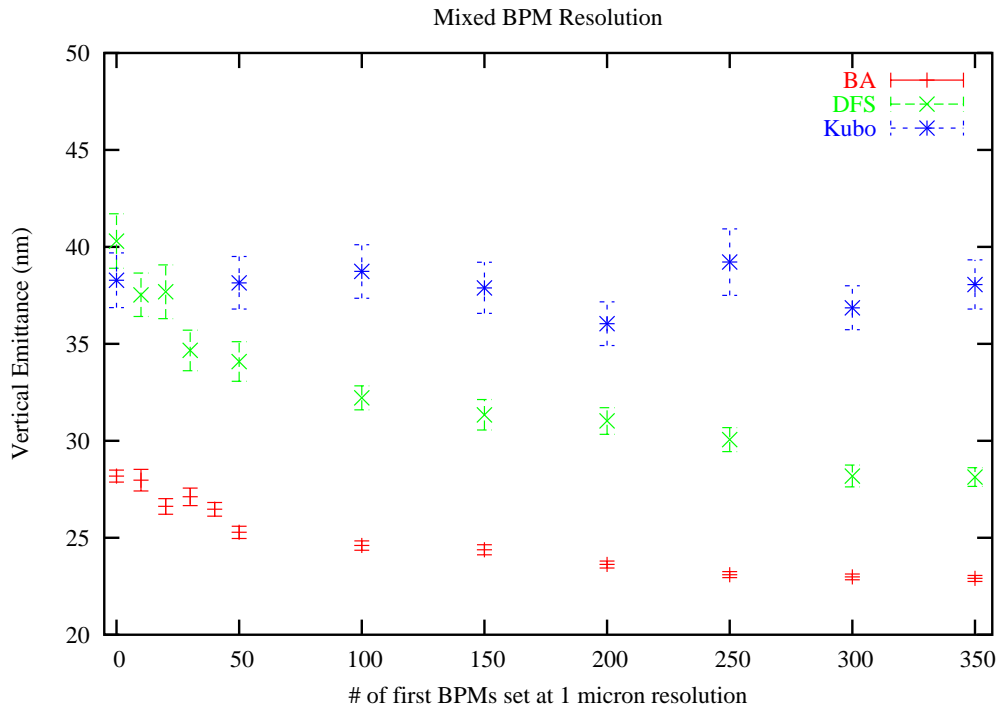


FIG. 3: The first part of the linac is set to 1 micron resolution, with the rest of the BPMs set at 20 microns. The mean values together with the errors on the mean are given for 100 seeds.

Another factor that might potentially lead to emittance growth is tilt in the BPMs, transversal in the x-y plane. TAO assumes by default no tilt, but offers the option of setting a non-zero RMS tilt in the BPM noise. We started in the range of μrad and mrad and observed no change in the emittance upon alignment. Hardly any increase was detected up to 0.5 rad tilt in case of BA and DFS, with a dramatic increase over the budget only beyond 1 radian [Figure 4]. Kubo makes an exception, going over the budget at 0.4 radians, but overall the three BBA algorithms are insensitive to BPM tilt in our range of interests (small fractions of a radian).

Again, the different response of the algorithms to BPM tilt could be accounted by the amplitude of the orbits used. When tilted, the monitors will read a slightly smaller apparent position, equal to the vertical projection of the actual position. From geometrical considerations, the difference between the real position and the reading would directly depend on the magnitude of the tilt Φ :

$$\delta y = y(1 - \cos\Phi) \quad (4)$$

This difference should roughly match the effective BPM noise resolution (the resolution at which the emittance starts to exceed the 100% budget of 40 nm). Since the corrections applied in Kubo do not limit the orbit, greater offset in position (larger orbit amplitude) and quicker response to increasing tilt are detected. Conversely, with BA, adjusting the orbit

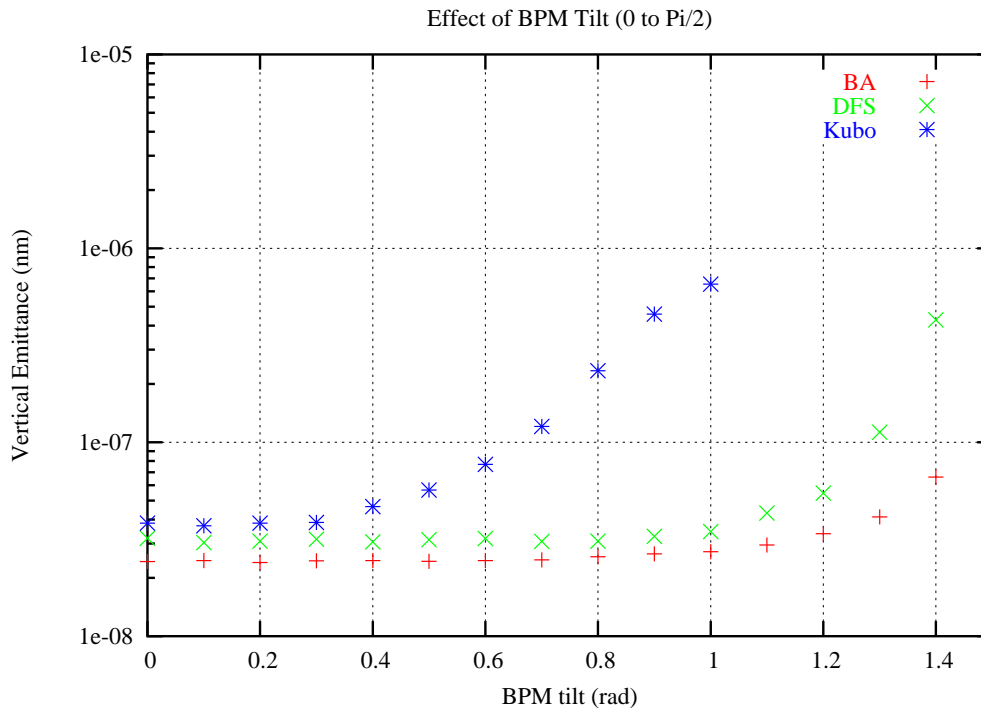


FIG. 4: Response to tilt in the BPMs, comparison for 100 seeds.

to match the ballistic track, one should expect a smaller orbit and consequently a larger tilt to get any noticeable increase in emittance. DFS seems to ultimately give the slowest response to tilt, possibly as a result of the corrections applied on the dispersive orbit. Also, the smallest orbit amplitude is recorded in this case.

IV. CORRELATIONS WITH DISPERSION

A further interesting exercise¹ is to track the vertical emittance across the linac for only one seed, with the lattice and beam priorly misaligned and the alignment algorithms applied. As in Figure 1, where the average over 100 seeds was plotted, there is a noticeable overall increasing trend; however, the smoothness is replaced by oscillations around an average curve, which does not necessarily match the 100 seeds curve. Upon plotting concomitantly the vertical dispersion function, which relates together both the position and the energy of the particles in the bunch, we have noticed a very similar pattern followed by the envelope of this dispersion function, with many peaks and sudden changes being closely correlated to similar changes in the projected emittance. As a result, one should always associate a significant emittance growth with an increase in dispersion, since the two notions are deeply intertwined; in both cases, one has an idea of how much the particles in the bunch get spread transversally, in both position and momentum/energy. The following graphs (Figure 5, 6, 7) are given to illustrate the connection just outlined.

Here we can see how the effort of stabilizing the beam and reaching a constant level for the emittance is closely matched by the decreasing trend in the envelope of the dispersion

¹ Study suggested by Dr. Andy Wolsky

function, towards the end of the linac.

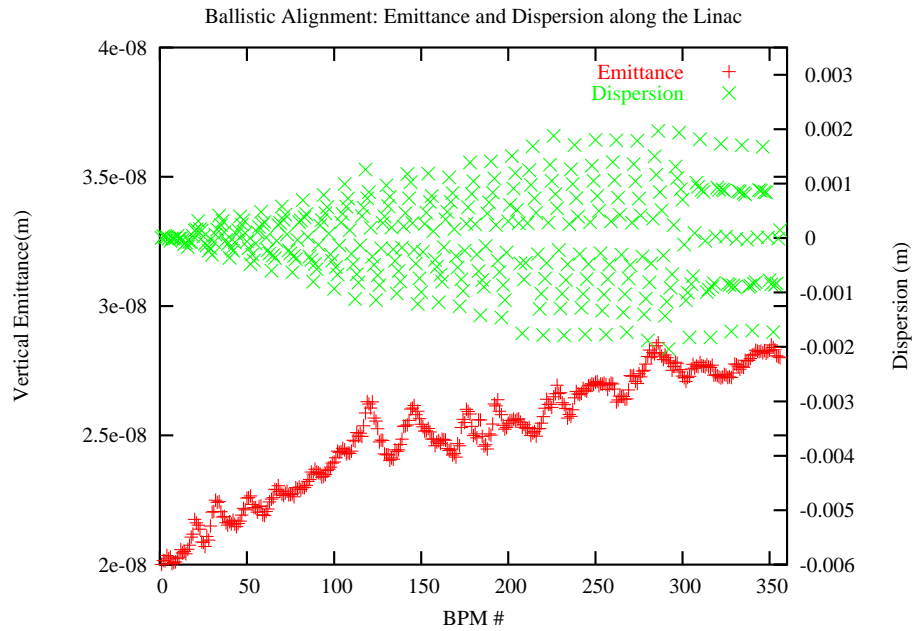


FIG. 5: The envelope of the dispersion matches the vertical emittance function; 1 seed only.

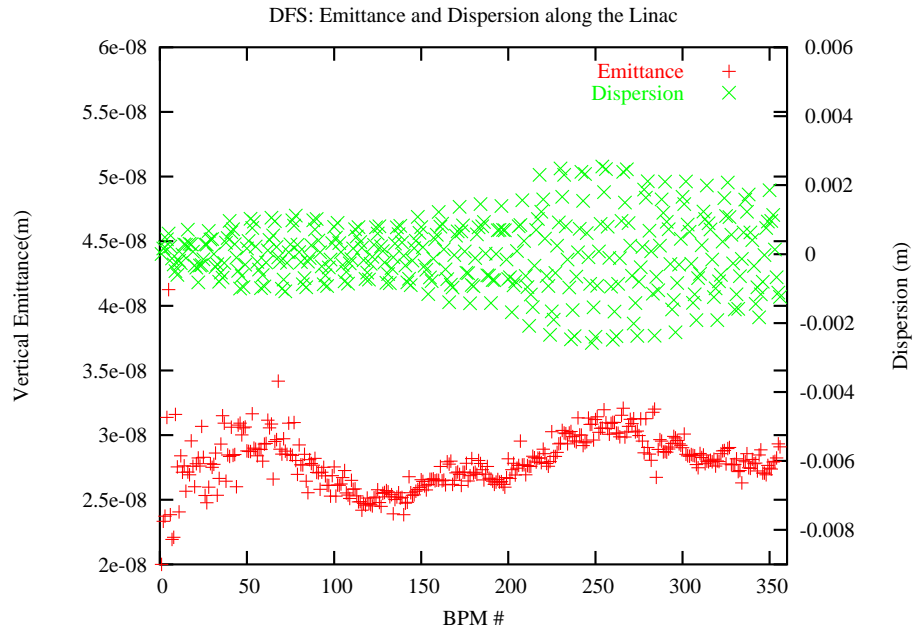


FIG. 6: The envelope of the dispersion matches the vertical emittance function; 1 seed only.

In other words, it turns out there is a fairly intimate connection between dispersion (largely determined by the lattice) and emittance (a characteristic of the beam), mostly because the largest source of emittance growth really comes from dispersion. While DFS aims directly at minimizing the dispersion when the alignment is performed, the other two algorithms attempt to reduce the dispersion as well, but in an indirect manner, by compensating

for any source of dispersion and adjusting any misalignments in the lattice. *Chromaticity*, a measure of how the focusing of the beam depends on the particle's momentum deviation, also comes into play here, but it can in principle be locally corrected by adjacent sextupoles [1].

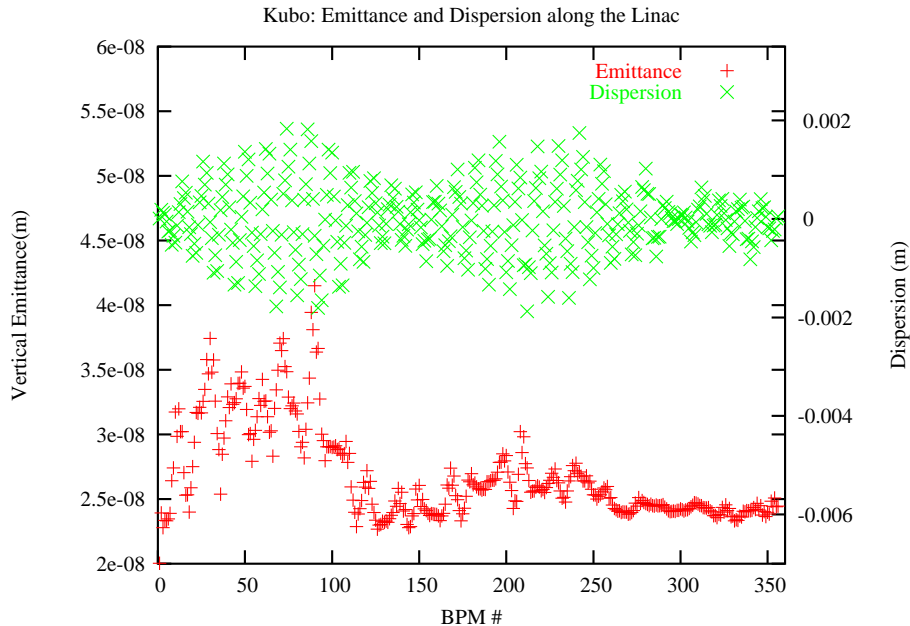


FIG. 7: The envelope of the dispersion matches the vertical emittance function; 1 seed only.

V. POSSIBLE IMPROVEMENTS TO THE ALIGNMENT ALGORITHMS

Some of the standard parameters in the three BBA algorithms already in use at Cornell have no strong theoretical or experimental support - first, a facility with a similar design has not yet been built, making impossible any reliable experimental feedback, and second, there are too many elements in the lattice subject to misalignments, which makes it difficult to predict the emittance growth with accuracy just from the fundamental laws of dynamics and electro-magnetism. Therefore, the numerical values for certain parameters have been found by simulation alone (many particle tracking), in an effort to minimize the final vertical emittance in the linac [2].

In the case of *Ballistic Alignment*, we directed our attention towards the number of FODO cells in a region. Given that all guide-field components are switched off in a single region, within which the beam is allowed to drift in a straight line, while the optics are restored to re-steer the beam on the reference ballistic path within that region alone, one should expect changes in the beam delivery according to differences in the configuration of regions. The standard in use has been 7 cells/region (with two quadrupoles in every cell). Figure 8 shows how the final vertical emittance changes if the number of cells in a region varies from 1 to 20. In particular, the very weak change in emittance for regions anywhere between 5 and 20 cells shows that we can easily work with fewer, longer regions, taking less time to realign the beam, with no additional emittance growth. The drawback to extending the length of the regions would come from losing some particles from the bunch as their trajectory gets

largely offset from the central axis (the whole bunch increases in size!), so considerations on the individual particles' orbits should ultimately decide where the line should be drawn.

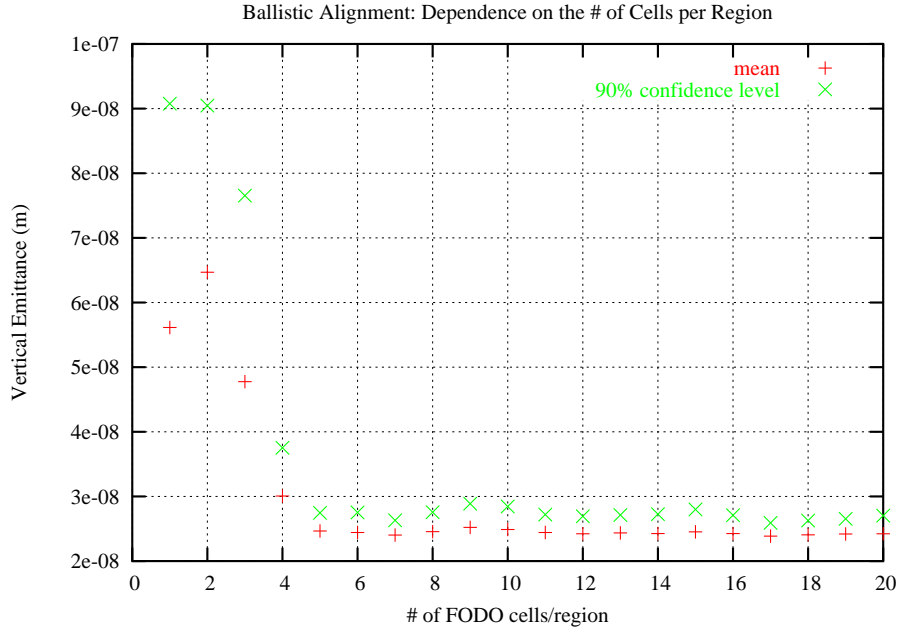


FIG. 8: Average over 100 seeds was considered; no significant change in the range 5 to 20 cells/region.

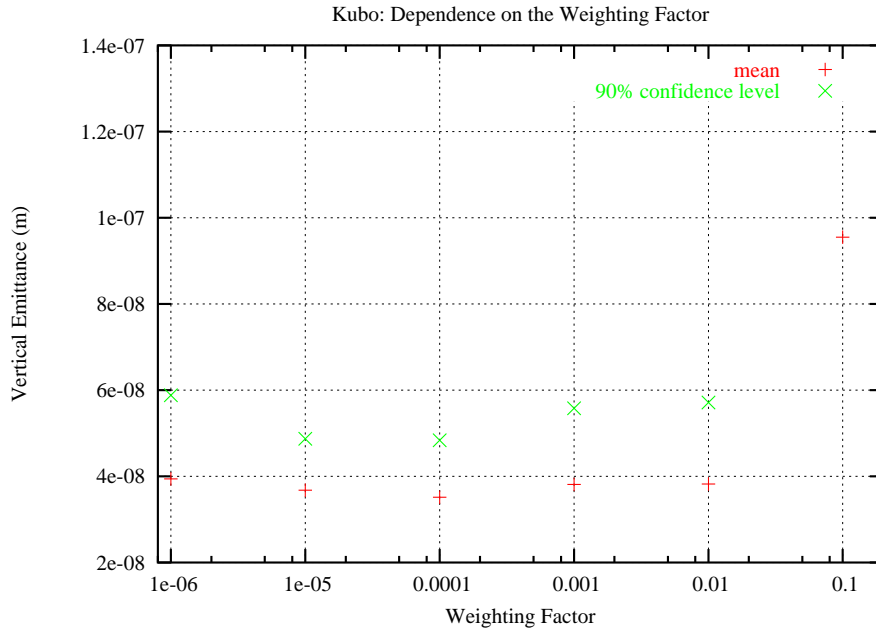


FIG. 9: Average over 100 seeds considered; 0.0001 might constitute an optimum.

In case of the Kubo method, one parameter subject to adjustments is the weighting factor for driving the beam to the BPM center, when a kick on each steering magnet is applied to compensate for the quadrupole kick. In the version outlined in [3], minor improvements

have been obtained if we change the weighting factor from 10^{-2} to 10^{-4} , but overall in the range from 10^{-6} to 10^{-2} the variations in emittance are of the order of a few nanometers. Factors larger than 0.1 increase the final emittance considerably over the budget and have been left out from the analysis (Figure 9).

Additionally, one can also look at the behavior of Kubo when the RMS BPM to quadrupole offset is changed from the $30 \mu\text{m}$ initially suggested [7, 8] to other comparable values. This number being an unknown error of the BPM offset with respect to the field center of the quadrupole next to it, suggestions on its exact value should come from measurement, upon performing quadrupole shunting. Since there are concerns that $30 \mu\text{m}$ may be an overly optimistic value, Figure 10 is showing the (roughly linear) dependence of the emittance growth on this parameter, pointing out that the 100 % growth budget can rapidly be exceeded.

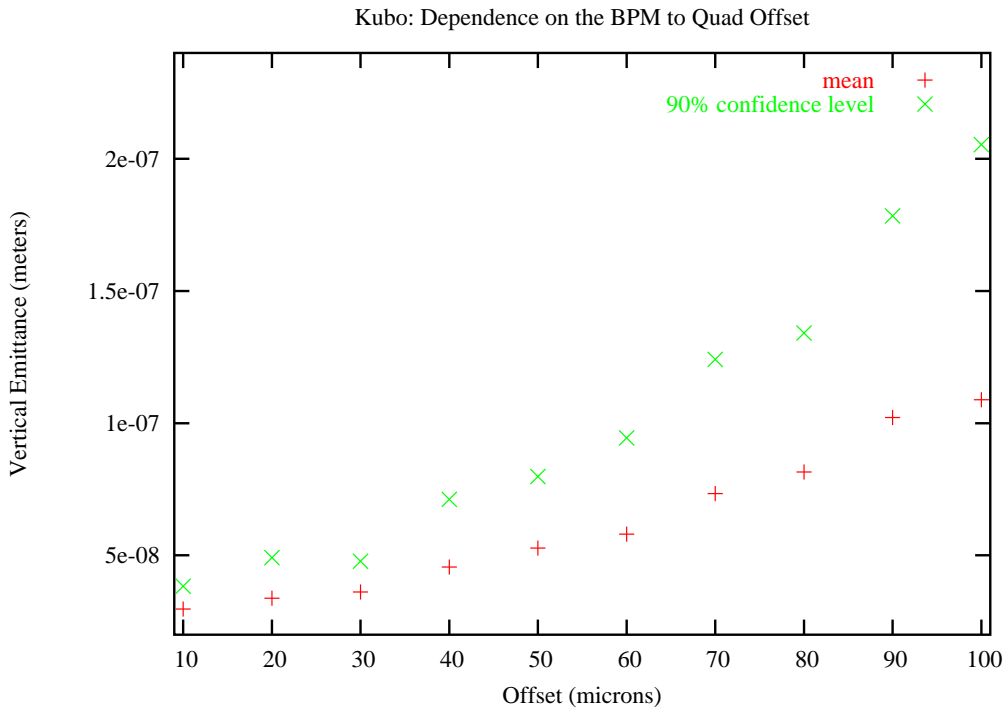


FIG. 10: Emittance growth with increasing BPM to quad offset; average taken over 100 seeds.

Finally, DFS is open to adjustments in both steering the beam to zero the BPMs and dividing the lattice into regions of FODO cells. In comparing the average final vertical emittance, together with the 90 % values and the statistical distribution of the 100 seeds in case of DFS performed with or without prior beam steering (histogram in Figure 11), it turns out that the differences are insignificant, so we might as well consider running the algorithm without the extra time-consuming beam steering process.

Another change in performance comes from dividing the lattice into regions with a different number of cells per region and a different cell overlap between adjacent regions. This bears importance in the fact that the trajectory is measured and adjusted by running an optimizer to minimize the dispersion on a particular region at once, moving progressively through the lattice to the next region. Figures 12 and 13 illustrate the change in emittance along the linac, pointing out that (1) having no overlap is inefficient because of various edge effects (a sudden shift in emittance can be seen every 40 BPM, that is, at the end of a 20

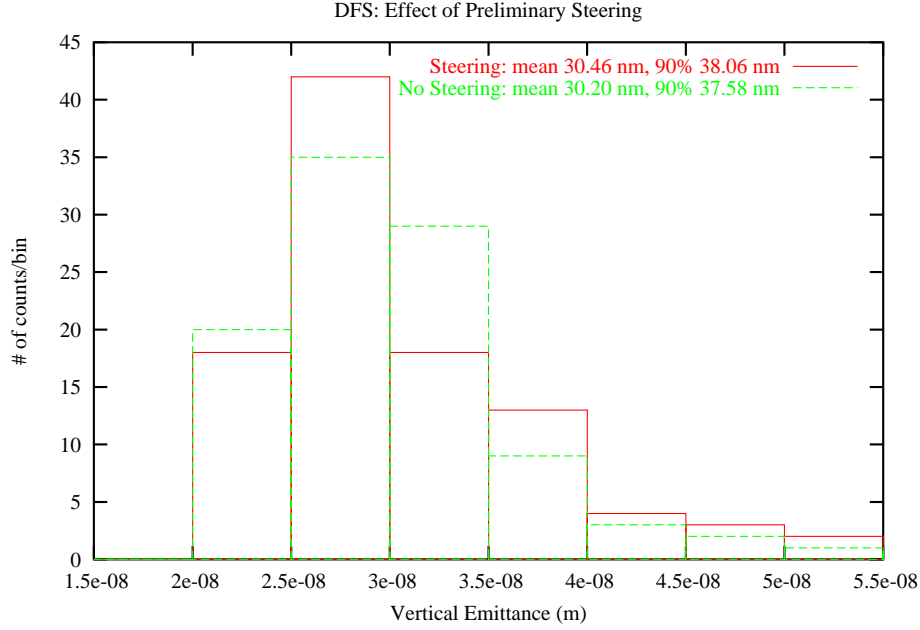


FIG. 11: Steering/no steering comparison; 100 points histogram.

cell region); (2) for a given length and a non-zero overlap, the higher the overlap, the greater the emittance; (3) certain configurations, such as 20/5 or 40/5 can prove more efficient in reducing the emittance than the standard 20 cells/10 overlap.

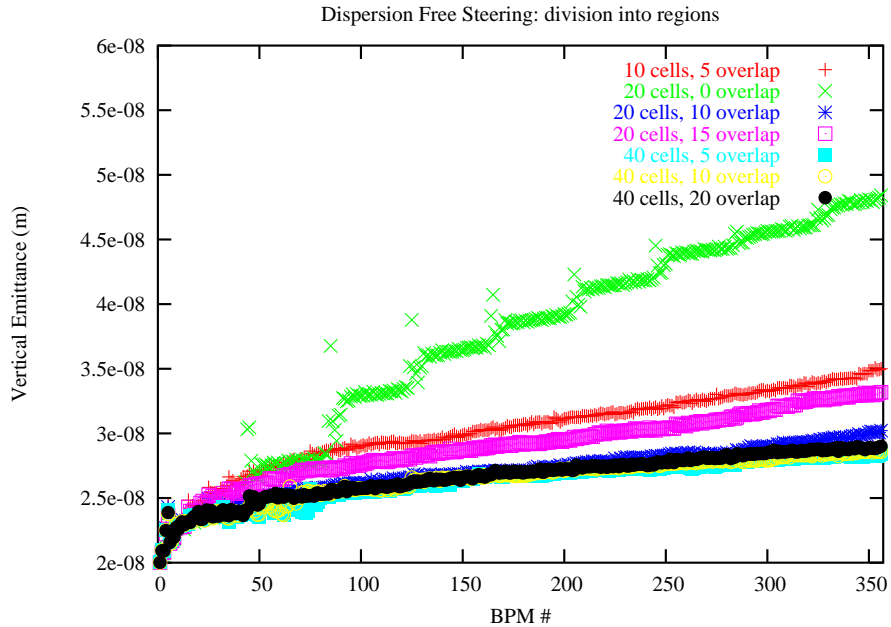


FIG. 12: Emittance is tracked throughout the linac (100 seeds). Optimum of 40 cells with 5 overlap found.

The difference in emittance can also be analyzed at variable BPM noise resolution (Figure 13). The qualitative comparison in efficiency between the 20/10 and 20/5 configurations still

holds when the monitor resolution is changed. As in the previous plots, the difference in emittance between different configurations are on the order of a few nanometers, but the fact that we applied the exact same initial conditions (not just random misalignments within the TESLA tolerance levels) suggests that the difference is real, and not just a result of statistical fluctuations. The errors on the mean are close to 1 nm.

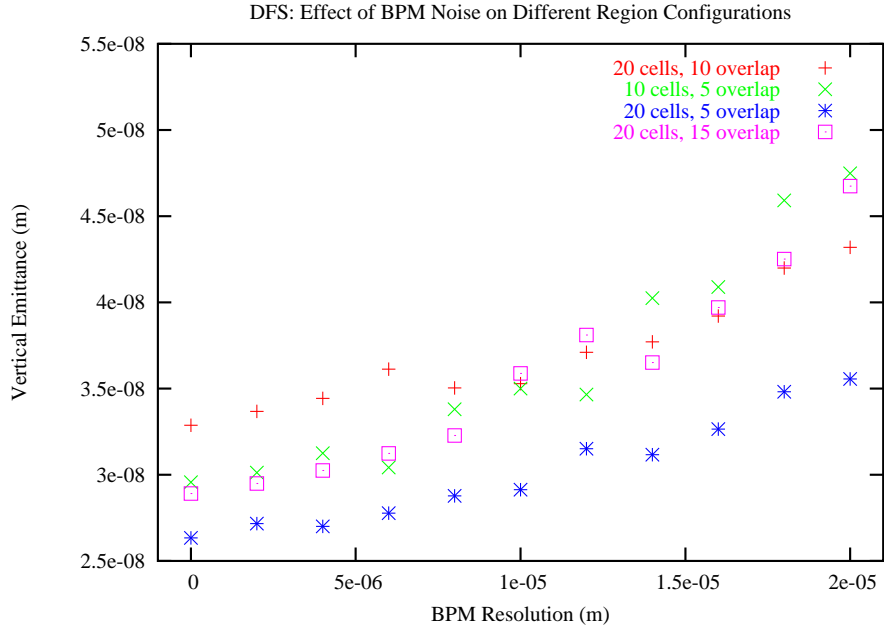


FIG. 13: The emittance behavior at variable monitor resolution points out the increased efficiency of a smaller non-zero overlap. Average over 100 seeds.

VI. CONCLUSIONS

The contributions of this study lie mainly in testing and comparing the performance of the beam-based alignment algorithms with results from previous versions and studies done at Cornell and elsewhere.

Mixed resolution considerations for the linac, the low response from Kubo to changing BPM resolution but a larger sensitivity to BPM tilt, the connection between dispersion and emittance and, ultimately, slight improvements brought to the algorithms by changing certain characteristic parameters, especially the division of the lattice into regions, are some of the highlights. We hope that all these suggestions can be wisely integrated in future versions of the algorithms, provided that other processes such as wakefields and decrease in dynamic aperture will not limit the extent to which the beam can handle alternate approaches without significant emittance growth. Integrative simulations that will take into account concomitantly beam jitter, stray fields, wakefields, BPM failure and ground motion, together with the various misalignments of the beam and lattice, should ultimately confirm the relative performance of the alignment algorithms and look for an overall efficient solution.

VII. ACKNOWLEDGEMENTS

I would like to thank Prof. David Rubin and graduate student Jeff Smith for setting up the framework for my summer research project. The latter is to be credited for implementing the BBA algorithms used by the Cornell Accelerator Group and other useful TAO routines, as well as providing continuous guidance throughout the project. Prof. Ritchie Patterson and Dr. Andy Wolsky were kind enough to come with helpful suggestions on extending the scope of the project and interpreting the results. Also, Prof. Rich Galik is to be thanked for facilitating this summer research opportunity. Lastly, I thank fellow student Kristin Kopp for the collaboration work and Prof. David Sagan for writing and providing assistance on the Bmad code, the parent software for TAO.

-
- [1] K. Wille, *The Physics of Particle Accelerators*, Oxford University Press (2000)
 - [2] J. Smith, *The Physics of the ILC Main Linac Emittance Dilution*, to be published (2005)
 - [3] J. Smith et al., *Comparison of Beam-Based Alignment Algorithms for the ILC*, Proc. PAC 05 (2005)
 - [4] J. Smith and D. Sagan, *The TAO Accelerator Simulation Program*, Proc. PAC 05 (2005)
 - [5] D. Schulte (CERN), *Emittance Preservation in the Main Linac of CLIC*, Stockholm, epaper.kek.jp/e98/PAPERS/MOP52C.PDF (1998)
 - [6] P. Tenenbaum R. Brinkmann, V. Tsakanov, *Beam-Based Alignment of the TESLA Main Linac*, SLAC-PUB-9264 (2002)
 - [7] K. Kubo (KEK), *Tolerances of misalignment of quads and cavities of ILC main linac*, lcdev.kek.jp/ILCAsiaNotes/2005/ILCAsia2005 (2005)
 - [8] K. Kubo, *Emittance dilution due to misalignment of quads and cavities of ILC main linac*, lcdev.kek.jp/ILCAsiaNotes/2005/ILCAsia2005-01.pdf (2005)
 - [9] TESLA: *Technical Design Report* (2001)
 - [10] T. Braşoveanu, K. Kopp, TAO simulations (2005)
 - [11] K. Ranjan, N. Solyak, S. Mishra (Fermilab) P.Tenenbaum, *Study of Main Linac Single Bunch Emittance Preservation in USColdLC Design (500 GeV CM)*, www-project.slac.stanford.edu/ilc/meetings/thursday/2005-05-05_UsColdLC.ppt (2005)